J. Fluid Mech. (1990), *vol.* 214, *pp.* 611–637
Printed in Great Britain

The inviscid axisymmetric stability of the supersonic flow along a circular cylinder

By PETER W. DUCK
Department of Mathematics, University of Manchester, Manchester M13 9PL, UK

(Received 9 January 1989 and in revised form 2 November 1989)

The supersonic flow past a thin straight circular cylinder is investigated. The associated boundary-layer flow (i.e. the velocity and temperature field) is computed; the asymptotic, far downstream solution is obtained, and compared with the full numerical results.

The inviscid, linear, axisymmetric (temporal) stability of this boundary layer is also studied. A so-called 'doubly generalized' inflexion condition is derived, which is a condition for the existence of so-called 'subsonic' neutral modes. The eigenvalue problem (for the complex wavespeed) is computed for two free-stream Mach numbers (2.8 and 3.8), and this reveals that curvature has a profound effect on the stability of the flow. The first unstable inviscid mode is seen to disappear rapidly as curvature is introduced, whilst the second (and generally the most important) mode suffers a substantially reduced amplification rate.

1. Introduction

The current and proposed development of high-speed flight vehicles has rekindled the general research effort into supersonic and hypersonic flows. One of the key areas of aerodynamic study is that of boundary-layer stability/transition to turbulence. In the case of compressible flow, Tollmien–Schlichting, Görtler and inviscid instabilities are all possible.

The problem of the stability of axisymmetric flows is of obvious relevance to flight vehicles, for example to the flow over fuselages, engine clowlings and small projectiles. In a recent paper Duck & Hall (1989) used triple-deck theory to consider the linear (and weakly nonlinear) viscous instability of an axisymmetric boundary layer in a supersonic flow to axisymmetric instabilities. It was found that viscous modes can exist in pairs (i.e. for a given body radius, there exist two neutral wavenumbers with two corresponding wavespeeds), and that at a given Mach number, such modes occur only for a body radius less than a critical value (dependent on Mach number).

In a second paper, Duck & Hall (1990) went on to consider non-axisymmetric viscous disturbances. These were generally found to be more important than axisymmetric viscous modes (possessing generally larger growth rates and occurring at larger body radii), whilst again it was found that neutral modes existed in pairs at body radii less than some critical value (dependent on the Mach number and azimuthal wavenumber).

However, it is generally found in the case of supersonic flows that inviscid disturbances are more important than viscous disturbances (this is in contrast to many incompressible flows where viscous instabilities are dominant).

One of the earliest attempts to study inviscid compressible stability was made by

Küchemann (1938); in this study, the temperature gradient and the curvature of velocity profile (together with the effects of viscosity) were both neglected, assumptions which it turns out cannot be properly justified. The work that provided a key to understanding this type of instability was Lees & Lin (1946), in which an asymptotic approximation was developed, analogous to the incompressible work of Lin (1945*a*, *b*, *c*). It was found that the quantity $(\partial/\partial y^*)(\rho^* \partial u^*/\partial y^*)$ (where u^* denotes the velocity tangential to the surface, y^* the coordinate normal to the surface, and ρ^* the fluid density) plays a key role, very similar to that of $\partial^2 u^*/\partial y^{*2}$ in incompressible theory, and as such may lead to a 'generalized inflexion point' type of instability if this quantity is zero. It was shown that unlike incompressible Blasius-type layers, the flat-plate compressible boundary layer can be unstable to purely inviscid modes. This (two-dimensional) work on compressible boundary layers was then extended to three dimensions by Reshotko (1962).

However, the major differences between incompressible and compressible theory were not fully uncovered until extensive numerical calculations were possible. The first of these, by Brown (1962), was followed by a series of computational studies by Mack (1963, 1964, 1965*a*, *b*, 1969, 1984, 1987). A further important difference with incompressible results was then revealed, namely that compressible theory predicts an infinite sequence of additional modes. These are referred to as higher modes, and are of great importance for boundary layers since it is the first of these (the so-called second mode) that is often the most unstable according to inviscid theory.

In the light of this numerical work, the prediction of Lees (1947), that cooling the wall acts to stabilize the boundary layer, turns out to be a little misleading (cooling can actually destabilize the flow, according to Mack 1969, 1984, 1987); in this case, although the 'generalized inflexion point' of the profile may disappear with cooling, these additional modes persist.

In the light of this work on planar boundary layers, we now turn to consider the inviscid axisymmetric stability of the boundary layer on a straight circular cylinder, the generators of the cylinder lying parallel to the flow. In particular we wish to investigate the effect curvature plays on the stability of the flow, and so we postulate that (generally) the radius of the body is of the same order of thickness as the boundary layer. Consistent with this we choose to prescribe planar conditions at the 'leading edge' of the cylinder, although the techniques to be described could be readily extended to other leading-edge conditions (e.g. 'rounded tips'). This approach may be fully justified if we restrict our attention to thin cylinders.

2. Equations of motion/state

We take the z^* axis to coincide with the axis of the cylinder, r^* the radial coordinate, and θ the azimuthal angle. a^* is the radius of the cylinder, which is taken to be independent of both z^* and θ. The velocity vector is taken to be $\boldsymbol{v}^* = (v_1^*, v_2^*, v_3^*)$ in the (r^*, θ, z^*) directions respectively, and T^* to be the temperature of the fluid. Throughout we assume the flow to be completely independent of θ, and it is also assumed that the azimuthal velocity component $v_2^* = 0$. The (full) equations (in the cylindrical system) of continuity, momentum and energy, are, respectively (see Thompson 1972)

$$\frac{\partial \rho^*}{\partial t^*} + \frac{\partial}{\partial r^*}(\rho^* v_1^*) + \frac{\rho^* v_1^*}{r^*} + \frac{\partial}{\partial z^*}(\rho^* v_3^*) = 0, \tag{2.1}$$

$$\rho^* \frac{\mathrm{D}v_1^*}{\mathrm{D}t^*} = -\frac{\partial p^*}{\partial r^*} + \frac{\partial \Sigma_{r^*r^*}}{\partial r^*} + \frac{\partial \Sigma_{r^*z^*}}{\partial z^*} + \frac{1}{r^*}\Sigma_{r^*r^*}, \tag{2.2}$$

$$\rho^* \frac{\mathrm{D}v_3^*}{\mathrm{D}t^*} = -\frac{\partial p^*}{\partial z^*} + \frac{\partial \Sigma_{z^*r^*}}{\partial r^*} + \frac{\partial \Sigma_{z^*z^*}}{\partial z^*} + \frac{1}{r^*}\Sigma_{z^*r^*}, \tag{2.3}$$

$$\rho^* \frac{\mathrm{D}}{\mathrm{D}t^*}(c_p T^*) - \frac{\mathrm{D}p^*}{\mathrm{D}t^*} = \Gamma^* + \frac{1}{r^*}\frac{\partial}{\partial r^*}\left(K^* r^* \frac{\partial T^*}{\partial r^*}\right) + \frac{\partial}{\partial z^*}\left(K^* \frac{\partial T^*}{\partial z^*}\right). \tag{2.4}$$

Here ρ^* denotes the density of the fluid, p^* the pressure, c_p the specific heat at constant pressure, K^* the coefficient of heat conductivity. The Eulerian operator is defined as

$$\frac{\mathrm{D}}{\mathrm{D}t^*} = \frac{\partial}{\partial t^*} + v_1^* \frac{\partial}{\partial r^*} + v_3^* \frac{\partial}{\partial z^*}, \tag{2.5}$$

and the viscous stress components (assuming Newtonian flow) are

$$\Sigma_{r^*r^*} = 2\mu^* \frac{\partial v_1^*}{\partial r^*} + \lambda^* \nabla \cdot \boldsymbol{v}^*, \tag{2.6}$$

$$\Sigma_{z^*z^*} = 2\mu^* \frac{\partial v_3^*}{\partial z^*} + \lambda^* \nabla \cdot \boldsymbol{v}^*, \tag{2.7}$$

$$\Sigma_{r^*z^*} = \Sigma_{z^*r^*} = \mu^* \left[\frac{\partial v_3^*}{\partial r^*} + \frac{\partial v_1^*}{\partial z^*}\right]. \tag{2.8}$$

The dispersion function Γ^* is defined to be

$$\Gamma^* = 2\mu^*[D_{r^*r^*}^2 + D_{z^*z^*}^2 + 2D_{z^*r^*}^2] + (\lambda^* - \tfrac{2}{3}\mu^*)(\nabla \cdot \boldsymbol{v}^*)^2, \tag{2.9}$$

where the rate-of-deformation tensors are

$$D_{r^*r^*} = \frac{\partial v_1^*}{\partial r^*}, \tag{2.10}$$

$$D_{z^*z^*} = \frac{\partial v_3^*}{\partial z^*}, \tag{2.11}$$

$$D_{r^*z^*} = \frac{1}{2}\left(\frac{\partial v_1^*}{\partial z^*} + \frac{\partial v_3^*}{\partial r^*}\right). \tag{2.12}$$

μ^* denotes the first coefficient of viscosity, and λ^* the bulk viscosity.

We now go on to assume a perfect gas equation of state, namely

$$p^* = \rho^* R^* T^* \tag{2.13}$$

(where R^* is the gas constant). We also assume that μ^* is solely a function of T^* (to be prescribed later).

The surface of the cylinder lies along $r^* = a^*$, $z^* \geqslant 0$, along which we set $\boldsymbol{v}^* = \boldsymbol{0}$. If we assume that the surface of the cylinder is insulated, then

$$\left.\frac{\partial T^*}{\partial r^*}\right|_{r^*=a^*} = 0. \tag{2.14}$$

Conditions at $z^* = 0$ must be specified. For the purposes of this paper, we assume that the boundary layer at $z^* = 0$ has zero thickness implying that planar conditions prevail (for which a similarity solution exists, which therefore provides a universal upstream boundary condition); a similar assumption was made by Seban & Bond (1951) and their comments regarding this assumption are valid here. Further, since

the cylinder is taken to be straight and thin, to leading order the far field is taken to be uniform, with velocity vector $(0, 0, U_\infty^*)$. The problem is now formally closed, and in the following section we go on to consider the basic boundary-layer flow on the surface of the cylinder, obtained by an approximation of the governing equations detailed above.

3. The basic flow

3.1. *The boundary-layer approximation*

Here we consider the steady boundary-layer approximation for the basic flow, derived from (1.1)–(1.4). A fundamental (and important) component of this paper is the inclusion of curvature terms in the governing equations; we achieve this by generally taking the body radius to be of the same order as the boundary-layer thickness (a similar approach was adopted by, for example, Seban & Bond 1951; Glauert & Lighthill 1955; Stewartson 1955; Bush 1976; and Duck & Bodonyi 1986).

With the formation of a thin boundary layer (comparable in thickness with the body radius) we expect the following classical assumptions to hold:

$$\frac{\partial}{\partial r^*} \gg \frac{\partial}{\partial z^*}, \tag{3.1}$$

and

$$v_3^* \gg v_1^* \tag{3.2}$$

(these orders will be made more precise shortly).

We take c_p to be a constant, the pressure to be uniform everywhere (if transverse pressure gradients are insignificant). Our crucial assumption (for the purposes of this study) is that the body radius is of the same order as the boundary-layer thickness, i.e. very thin. One further important consequence of neglecting transverse pressure gradients is that the equation of state may be written in the following form:

$$\rho^* T^* = \rho_\infty^* T_\infty^*, \tag{3.3}$$

where subscript ∞ denotes free-stream conditions.

We also require a relationship linking the viscosity μ^* to temperature T^*. Here we take the simplest form, namely the linear Chapman law (see Stewartson 1964), i.e.

$$\frac{\mu^*}{\mu_\infty^*} = \frac{CT^*}{T_\infty^*}, \tag{3.4}$$

where C is the Chapman constant (although, here, conceptually, there would be no difficulty incorporating more complex viscosity/temperature laws).

It is now convenient to introduce non-dimensional quantities:

$$(v_1, v_3, r, z, T, \rho, \mu) = \left(\frac{C^{-1} Re\, v_1^*}{U_\infty^*}, \frac{v_3^*}{U_\infty^*}, \frac{r^*}{a^*}, \frac{C Re^{-1} z^*}{a^*}, \frac{T^*}{T_\infty^*}, \frac{\rho^*}{\rho_\infty^*}, \frac{\mu^*}{\mu_\infty^*}\right), \tag{3.5}$$

where Re is the Reynolds number, based on body radius a^*, namely

$$Re = \frac{U_\infty^* a^* \rho_\infty^*}{\mu_\infty^*}, \tag{3.6}$$

which must be assumed large if the assumptions (3.1) and (3.2) are to be valid.

Equations (1.1)–(1.4) may then be written in the following non-dimensional form:

$$\frac{\partial}{\partial r}\left(\frac{v_1}{T}\right)+\frac{v_1}{rT}+\frac{\partial}{\partial z}\left(\frac{v_3}{T}\right)=0, \tag{3.7}$$

$$\frac{\partial p}{\partial r}=0, \tag{3.8}$$

$$v_1\frac{\partial v_3}{\partial r}+v_3\frac{\partial v_3}{\partial z}=\frac{T}{r}\frac{\partial}{\partial r}\left(rT\frac{\partial v_3}{\partial r}\right), \tag{3.9}$$

$$v_1\frac{\partial T}{\partial r}+v_3\frac{\partial T}{\partial z}=T^2(\gamma-1)M_\infty^2\left(\frac{\partial v_3}{\partial r}\right)^2+\frac{T}{r}\frac{\partial}{\partial r}\left(\frac{rT}{\sigma}\frac{\partial T}{\partial r}\right). \tag{3.10}$$

Here σ is the Prandtl number, namely

$$\sigma=\frac{\mu^* c_p}{K^*}, \tag{3.11}$$

which in this paper we shall assume to be a constant; γ is the ratio of specific heats, and M_∞ the Mach number, namely

$$M_\infty=\frac{U_\infty^*}{(\gamma R^* T_\infty^*)^{\frac{1}{2}}}. \tag{3.12}$$

The boundary conditions are (in the insulated wall case)

$$\left.\begin{aligned}&\left.\frac{\partial T}{\partial r}\right|_{r=1}=0,\\ &v_1=v_3=0 \quad \text{on} \quad r=1,\\ &\left.\begin{aligned}v_3&\to 1\\ T&\to 1\end{aligned}\right\} \quad \text{as} \quad r\to\infty.\end{aligned}\right\} \tag{3.13}$$

The problem is now closed, and we next consider its numerical solution.

3.2. *Numerical solution*

As $z\to 0$ we specify that conditions become planar (Stewartson 1964) and so we expect the solution to become singular. This latter condition renders the problem in its present form inappropriate for numerical treatment. Instead we write

$$v_1=\zeta^{-1}\hat{v}_1(\eta,\zeta), \quad v_3=\hat{v}_3(\eta,\zeta), \quad T=\hat{T}(\eta,\zeta), \tag{3.14}$$

with

$$\zeta=z^{\frac{1}{2}}, \quad \eta=(r-1)/\zeta. \tag{3.15a, b}$$

The 'hatted' functions are now expected to be completely regular as $\zeta\to 0$, approaching their planar counterparts. Equations (3.7), (3.9), (3.10) then become, respectively,

$$\hat{T}\hat{v}_{1\eta}-\hat{v}_1\hat{T}_\eta-\tfrac{1}{2}\eta\hat{T}\hat{v}_{3\eta}+\tfrac{1}{2}\zeta\hat{T}v_{3\zeta}+\tfrac{1}{2}\eta\hat{T}_\eta\hat{v}_3-\tfrac{1}{2}\zeta\hat{v}_3\hat{T}_\zeta+\frac{\zeta\hat{T}\hat{v}_1}{1+\eta\zeta}=0, \tag{3.16}$$

$$\hat{v}_1\hat{v}_{3\eta}-\tfrac{1}{2}\eta\hat{v}_3\hat{v}_{3\eta}+\tfrac{1}{2}\zeta\hat{v}_3\hat{v}_{3\zeta}=\hat{T}^2\left[\hat{v}_{3\eta\eta}+\frac{\zeta\hat{v}_{3\eta}}{1+\zeta\eta}\right]+\hat{T}\frac{\partial\hat{T}}{\partial\eta}\hat{v}_{3\eta}, \tag{3.17}$$

$$\hat{v}_1\hat{T}_\eta-\tfrac{1}{2}\eta\hat{v}_3\hat{T}_\eta+\tfrac{1}{2}\zeta\hat{T}_\zeta\hat{v}_3=\hat{T}^2(\gamma-1)M_\infty^2(\hat{v}_{3\eta})^2+\frac{\hat{T}}{\sigma}(\hat{T}_\eta)^2+\frac{\hat{T}^2}{\sigma}\hat{T}_{\eta\eta}+\frac{\hat{T}^2\zeta}{\sigma(1+\zeta\eta)}\hat{T}_\eta, \tag{3.18}$$

subject to

$$\left.\begin{aligned} &\hat{T}_\eta = 0 \quad \text{on} \quad \eta = 0, \quad \hat{v}_1 = \hat{v}_3 = 0 \quad \text{on} \quad \eta = 0, \\ &\hat{T} \to 1 \quad \text{as} \quad \eta \to \infty, \quad \hat{v}_3 \to 1 \quad \text{as} \quad \eta \to \infty. \end{aligned}\right\} \tag{3.19}$$

It is possible to define a stream function which would ensure that the continuity equation (3.16) is always satisfied; however, in this case, in addition to the order of the momentum equation being increased, the coefficients of the equations become considerably more complicated. Further, it does not appear possible to introduce a Howarth–Dorodnitsyn (Stewartson 1951; Moore 1955) like transformation which in the planar case considerably simplifies the governing equations. For this reason it was decided to seek a numerical solution to $\hat{v}_1$, $\hat{v}_3$ and $\hat{T}$ directly. Notice that setting $\zeta = 0$ reduces the system (3.16)–(3.19) to the planar problem, namely the ordinary differential system

$$\hat{T}\hat{v}_{1\eta} - \hat{v}_1\hat{T}_\eta - \tfrac{1}{2}\eta\hat{T}\hat{v}_{3\eta} + \tfrac{1}{2}\eta\hat{T}_\eta\hat{v}_3 = 0, \tag{3.20}$$

$$\hat{v}_1\hat{v}_{3\eta} - \tfrac{1}{2}\eta\hat{v}_3\hat{v}_{3\eta} = \hat{T}^2\hat{v}_{3\eta\eta} + \hat{T}\hat{T}_\eta\hat{v}_{3\eta}, \tag{3.21}$$

$$\hat{v}_1\hat{T}_\eta - \tfrac{1}{2}\eta\hat{v}_3\hat{T}_\eta = \hat{T}^2(\gamma-1)M_\infty^2(\hat{v}_{3\eta})^2 + \frac{\hat{T}^2}{\sigma}\hat{T}_{\eta\eta} + \frac{\hat{T}}{\sigma}(\hat{T}_\eta)^2 \tag{3.22}$$

(again subject to (3.19)).

The variables

$$\hat{v}_3^1 = \hat{v}_{3\eta}, \quad \hat{T}^1 = \hat{T}_\eta, \tag{3.23}$$

were introduced, and the system (3.20)–(3.22) together with (3.23) were written as a system of first-order ordinary differential equations, which were then approximated by second-order finite differences. The truncated system was then solved by means of Newton iteration. At each iteration level, the algebraic system was of block-diagonal form, with each block comprising 10×5 elements.

Once the above solution was obtained, the system (3.16)–(3.19) was treated in much the same way, with a Crank–Nicolson approximation being used to approximate ζ-derivatives (again the problem was treated as a system of first-order equations in η). In this way, the solution was extended forwards in ζ.

Figure 1(*a*) shows the distribution of $\zeta^{-1}\hat{v}_{3\eta}(\eta = 0)$ with ζ, and figure 1(*b*) the corresponding distribution of $\hat{T}(\eta = 0)$. These results are for $M_\infty = 2.8$, with fluid constants $\sigma = 0.72$, $\gamma = 1.4$. The $\zeta^{-1}\hat{v}_{3\eta}(\eta = 0)$ distribution is singular in the planar limit as $\zeta \to 0$, and then appears to (slowly) fall continuously as ζ increases. The $\hat{T}(\eta = 0)$ distribution declines slightly from its planar value at $\zeta = 0$.

Results for $M_\infty = 3.8$ (same fluid constants as above) are shown in figure 2(*a*) ($\zeta^{-1}\hat{v}_3(\eta = 0)$ distribution) and figure 2(*b*) ($\hat{T}(\eta = 0)$ distribution); these suggest the same basic characteristics as the lower-Mach-number results.

The limit as $\zeta \to \infty$ is of some interest. Although, as indicated earlier, the incompressible case in this limit is well documented, the particular details for the compressible case do not appear to have been described, although Stewartson (1964) speculates that a similar approach to the incompressible case is necessary. In the following sub-section we show to a certain extent, that this is the case.

3.3. *The far downstream flow*

We find it convenient to reconsider the system (3.7)–(3.10) (together with (3.13)) when studying the limit of $z \to \infty$. The incompressible work of Glauert & Lighthill (1955), Stewartson (1955) and Bush (1976) suggests that two radial lengthscales are

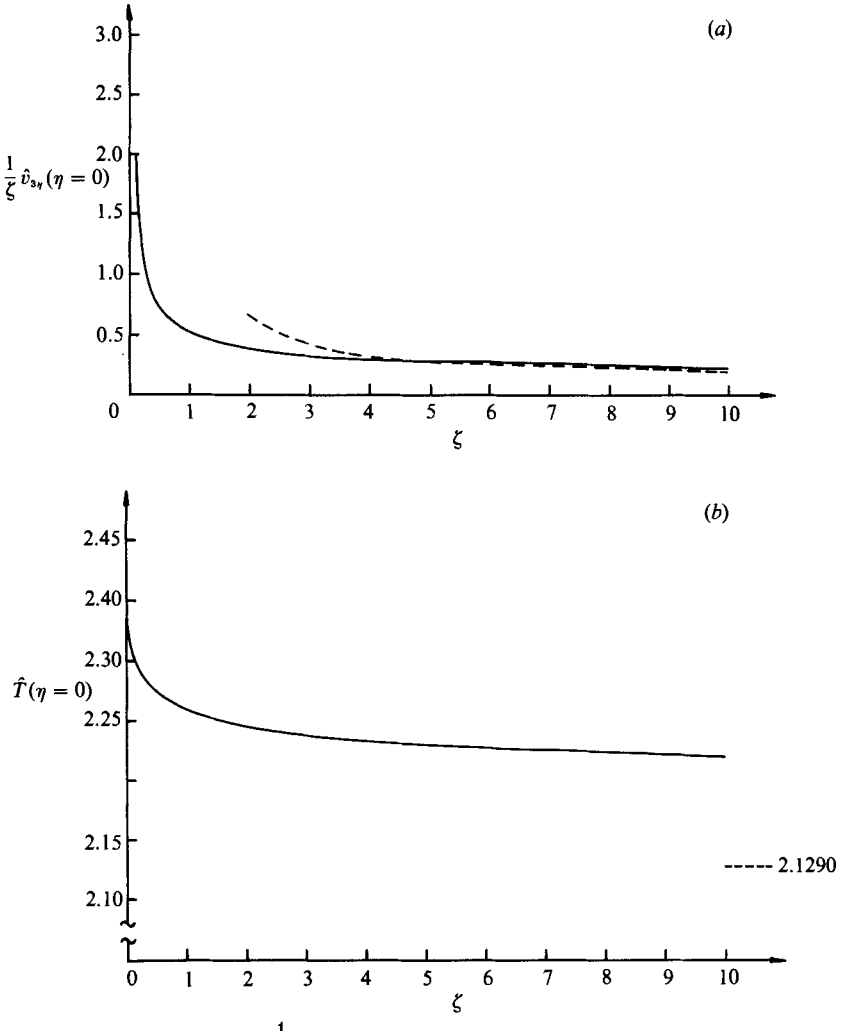

FIGURE 1. (*a*) Variation of $\frac{1}{\zeta}\hat{v}_{3\eta}(\eta=0)$ with ζ; (*b*) variation of $\hat{T}(\eta=0)$ with ζ. $M_\infty = 2.8$.

important in this limit, namely $r = O(1)$ and $r = O(z^{\frac{1}{2}})$. Following these earlier works, we find it convenient to define the parameter

$$\begin{aligned}\epsilon &= (\tfrac{1}{2}\log z)^{-1} \\ &= (\log\zeta)^{-1},\end{aligned} \tag{3.24}$$

which is necessarily small as $z \to \infty$.

Guided partly by the incompressible case, we expect the solution for $r = O(1)$ to take the following form:

$$v_1 = O(1/\zeta), \tag{3.25a}$$

$$v_3 = \epsilon\bar{v}_3(r,\epsilon) + O(1/\zeta), \tag{3.25b}$$

$$T = \bar{T}_0(r,\epsilon) + O(1/\zeta), \tag{3.25c}$$

where quantities with an overbar are expected to be generally order one. We see

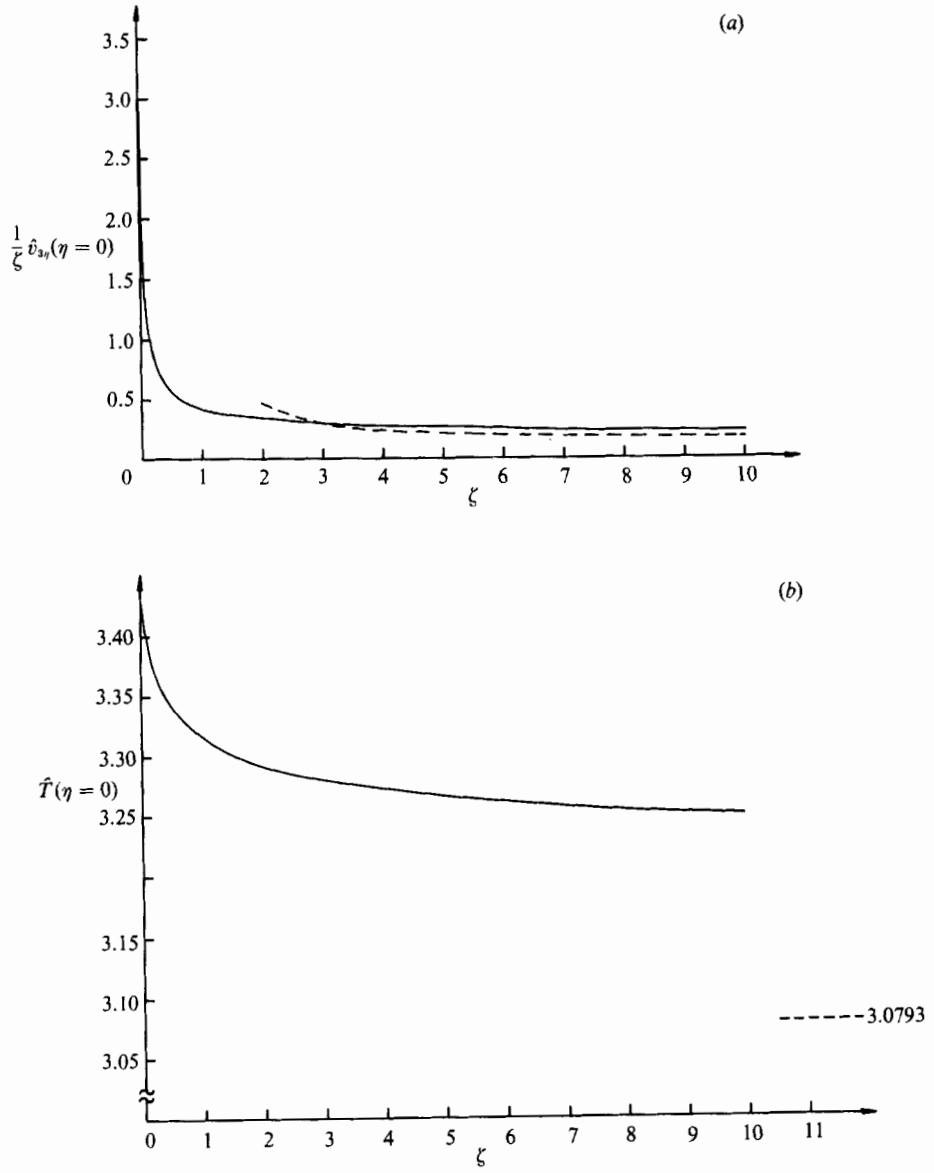

FIGURE 2. (*a*) Variation of $\frac{1}{\zeta}\hat{v}_{3\eta}(\eta=0)$ with ζ; (*b*) variation of $\hat{T}(\eta=0)$ with ζ. $M_\infty = 3.8$.

therefore that the corrections here are exponentially small in ϵ. Substitution of (3.25) into (3.7)–(3.10) immediately reveals the result (neglecting $O(1/\zeta)$ terms)

$$\frac{\partial}{\partial r}\left[r\bar{T}_0\frac{\partial \bar{v}_3}{\partial r}\right] = 0, \tag{3.26}$$

and

$$\bar{T}_0(\gamma-1)M_\infty^2\epsilon^2\left(\frac{\partial \bar{v}_3}{\partial r}\right)^2 + \frac{1}{r}\frac{\partial}{\partial r}\left(r\frac{\bar{T}_0}{\sigma}\frac{\partial \bar{T}_0}{\partial r}\right) = 0. \tag{3.27}$$

Integrating (3.26) yields

$$\bar{T}_0 \frac{\partial \bar{v}_3}{\partial r} = \frac{\bar{K}}{r}, \tag{3.28}$$

where $\bar{K}$ is independent of r. Substitution of (3.28) into (3.27) yields

$$\bar{T}_0 \frac{\partial}{\partial r}\left(r\bar{T}_0 \frac{\partial \bar{T}_0}{\partial r}\right) + \frac{(\gamma-1)\bar{K}^2 M_\infty^2 \epsilon^2 \sigma}{r} = 0. \tag{3.29}$$

To facilitate the solution to (3.29) we write

$$\bar{r} = \ln r, \tag{3.30}$$

and so

$$\bar{T}_0 \frac{\partial}{\partial \bar{r}}\left(\bar{T}_0 \frac{\partial \bar{T}_0}{\partial \bar{r}}\right) + \bar{K}^2 \sigma M_\infty^2 (\gamma-1)\epsilon^2 = 0. \tag{3.31}$$

This equation is further simplified by the use of a second transformation

$$\bar{R} = \int \frac{\mathrm{d}\bar{r}}{\bar{T}_0}, \tag{3.32}$$

which is effectively a Howarth–Dorodnitsyn transformation (Stewartson 1964), giving

$$\frac{\partial^2 \bar{T}_0}{\partial \bar{R}^2} + \bar{K}^2 M_\infty^2 \sigma(\gamma-1)\epsilon^2 = 0. \tag{3.33}$$

Consequently

$$\bar{T}_0 = -\tfrac{1}{2}\bar{K}^2 M_\infty^2 \sigma(\gamma-1)\epsilon^2 \bar{R}^2 + \epsilon A_0 \bar{R} + B_0, \tag{3.34}$$

where A_0 and B_0 are independent of $\bar{R}$, and are functions of ϵ only, such that A_0 and B_0 are (generally) $O(1)$ as $\epsilon \to 0$, i.e. we may write

$$\left.\begin{aligned} A_0 &= A_{00} + \epsilon A_{01} + \epsilon^2 A_{02} + O(\epsilon^3), \\ B_0 &= B_{00} + \epsilon B_{01} + \epsilon^2 B_{02} + O(\epsilon^3). \end{aligned}\right\} \tag{3.35}$$

Before proceeding further with this solution, we consider next the outer solution where $\eta = O(1)$. Guided by the above, and also again the corresponding incompressible results, we expect the solution to develop as

$$\left.\begin{aligned} v_3 &= 1 + \epsilon \tilde{v}_3(\bar{\eta}) + O(\epsilon^2), \\ T &= 1 + \epsilon \tilde{T}_3(\bar{\eta}) + O(\epsilon^2), \\ v_1 &= \epsilon \tilde{v}_1(\bar{\eta}) + O(\epsilon^2), \end{aligned}\right\} \tag{3.36}$$

where we have written,

$$\bar{\eta} = \int_0^\eta \frac{\mathrm{d}\eta}{T},$$

and also we have implemented free-stream conditions on v_3 and T.

If $\bar{T}_0(r, \zeta)$ is to match correctly to (3.35), we must have (to leading order in ϵ)

$$A_{00} + B_{00} - \tfrac{1}{2}\bar{K}^2 M_\infty^2 (\gamma-1)\sigma = 1 \tag{3.37}$$

(it is now clear that although the first term on the right-hand side of (3.34) is notionally $O(\epsilon^2)$, its inclusion is essential for a correct matching process, as is the second term). Note that we have used the result

$$\bar{R} \sim \bar{r} \sim \ln r \quad \text{as} \quad r \to \infty. \tag{3.38}$$

The matching of $\bar{v}_3(r, \zeta)$ with the outer solution is achieved by setting $\bar{K} = 1$.

The $O(\epsilon)$-corrections to (3.36) are then given by

$$\tilde{v}_3(\bar{\eta}) = \int_\infty^\eta \frac{\exp\left[-\frac{1}{2}\int\frac{\mathrm{d}\bar{\eta}}{\bar{T}}\right]}{\bar{\eta}}\mathrm{d}\bar{\eta}, \tag{3.39}$$

and

$$\tilde{T}_1(\bar{\eta}) = [A_{00}-\sigma(\gamma-1)M_\infty^2]\int_\infty^\eta \frac{\exp\left[-\frac{\sigma}{2}\int\frac{\mathrm{d}\bar{\eta}}{\bar{T}}\right]}{\bar{\eta}}\mathrm{d}\bar{\eta}. \tag{3.40}$$

Both $\bar{\eta}$ and $\bar{R}$ may be regarded as forms of 'optimal coordinates', as their use is essential for the correct matching of solutions.

To complete the problem, we now require to specify conditions on $r = 1$. In the insulated wall case, to which the bulk of this paper is devoted, we require

$$\left.\frac{\partial T}{\partial r}\right|_{r=1} = 0, \tag{3.41}$$

and so

$$A_0 = A_{00} = 0. \tag{3.42}$$

This implies that

$$\bar{T}_0|_{r=1} = 1+\tfrac{1}{2}\sigma(\gamma-1)M_\infty^2+O(\epsilon), \tag{3.43}$$

which leads to

$$\left.\frac{\partial\bar{v}_3}{\partial r}\right|_{r=1} = \frac{1}{1+\frac{1}{2}\sigma(\gamma-1)M_\infty^2}+O(\epsilon) \tag{3.44}$$

(on account of (3.28)).

These asymptotic results are indicated as broken lines on figures 1 and 2 for comparison with the full numerical results; the agreement is satisfactorily given the relative 'largeness' of the small parameter ϵ.

If on the other hand the surface of the cylinder is heated or cooled, i.e. $T|_{r=1}$ is specified (to be T_w say), then we must have

$$B_0 = T_\mathrm{w}, \tag{3.45}$$

and so to leading order

$$A_0 = 1+\tfrac{1}{2}\sigma(\gamma-1)M_\infty^2-T_\mathrm{w}, \tag{3.46}$$

giving

$$\left.\frac{\partial\bar{T}_0}{\partial r}\right|_{r=1} = \frac{\epsilon}{T_\mathrm{w}}[1+\tfrac{1}{2}\sigma(\gamma-1)M_\infty^2-T_\mathrm{w}]+O(\epsilon^2), \tag{3.47}$$

together with,

$$\left.\frac{\partial\bar{v}_3}{\partial r}\right|_{r=1} = \frac{1}{T_\mathrm{w}}+O(\epsilon). \tag{3.48}$$

In the following section we turn our attention to the inviscid instability of flows corresponding to the insulated-wall class.

4. Inviscid disturbances

4.1. *Disturbance equations*

We now seek to determine the effect of a small-amplitude disturbance on the basic flow described in the previous section, to determine whether growth/instability can occur. We impose a disturbance whose wavelength is generally comparable with that of the boundary-layer thickness and therefore also of the body radius ($O(a^*)$), in

which case the parallel flow approximation can be fully justified; this implies that the disturbance equations are all inviscid.

Specifically, at a fixed z-station, we write (for example)

$$v_1^* = \delta\bar{\alpha}U_\infty^*\,\tilde{v}(r)\,\mathrm{e}^{\mathrm{i}\bar{\alpha}(Z-ct)}, \tag{4.1}$$

$$v_3^* = U_\infty^*[w_0(r)+\delta\tilde{w}(r)\,\mathrm{e}^{\mathrm{i}\bar{\alpha}(Z-ct)}], \tag{4.2}$$

$$T^* = T_\infty^*[T_0(r)+\delta\tilde{T}(r)\,\mathrm{e}^{\mathrm{i}\bar{\alpha}(Z-ct)}], \tag{4.3}$$

$$p^* = \rho_\infty^* R^* T_\infty^*[1+\delta\tilde{p}(r)\,\mathrm{e}^{\mathrm{i}\bar{\alpha}(Z-ct)}], \tag{4.4}$$

where δ is some small (disturbance amplitude) parameter,

$$t = (U_\infty^*/a^*)\,t^*, \quad Z = z^*/a^*, \tag{4.5a, b}$$

and so the $Z = O(1)$ scale is very much shorter than the $z = O(1)$ scale, $\bar{\alpha}$ is the non-dimensional spatial wavenumber, and c the non-dimensional wavespeed, and

$$w_0(r) = \hat{v}_3(r,z), \quad T_0(r) = \hat{T}(r,z), \tag{4.6}$$

where $\hat{v}_3$ and $\hat{T}$ are as defined in §3.

Substituting (4.1)–(4.4) into (1.1)–(1.4) and (1.13), taking the $O(\delta)$-terms with the leading order in R and combining these equations yields the following disturbance equation (written in terms of η rather than r):

$$\phi_\eta+\frac{\zeta}{1+\zeta\eta}\phi-\frac{w_{0\eta}\phi}{w_0-c} = \frac{\mathrm{i}\tilde{p}}{\gamma M_\infty^2}\left[\frac{T_0-M_\infty^2(w_0-c)^2}{w_0-c}\right], \tag{4.7}$$

$$\frac{\mathrm{i}\alpha^2(w_0-c)}{T_0}\phi = -\frac{\tilde{p}_\eta}{\gamma M_\infty^2}, \tag{4.8}$$

where $\tilde{v} = \zeta\phi$, and $\bar{\alpha} = \alpha/\zeta$. Equations (4.7) and (4.8) may be combined to give

$$\frac{\mathrm{d}}{\mathrm{d}\eta}\left\{\frac{(w_0-c)\left(\phi_\eta+\dfrac{\zeta}{1+\zeta\eta}\phi\right)-w_{0\eta}\phi}{T_0-M_\infty^2[w_0-c]^2}\right\} = \frac{\alpha^2}{T_0}(w_0-c)\,\phi. \tag{4.9}$$

This equation is a form of the disturbance equation used in compressible jet studies (see for example Michalke 1971), and is very similar to the well-known planar inviscid equation (Lees & Lin 1946; Reshotko 1962; Mack 1984, for example), except for the inclusion of the single curvature term on the left-hand side of the equation; notice that allowing $\zeta\to 0$ retrieves the planar result.

On $\eta = 0$, we require

$$\phi(\eta = 0) = 0 \tag{4.10}$$

(the impermeability condition). The second condition is that ϕ is bounded as $\eta\to\infty$. This is achieved by taking the $\eta\to\infty$ limit of (4.9) (neglecting exponentially small terms, but retaining algebraically small terms to include the effects of curvature),

$$\phi_{\eta\eta}+\frac{\zeta\phi_\eta}{1+\zeta\eta}-\frac{\zeta^2\phi}{(1+\zeta\eta)^2} = \alpha^2[1-M_\infty^2(1-c)^2]\,\phi, \tag{4.11}$$

giving

$$\phi \sim \phi_\infty K_1\left\{\pm\alpha[1-M_\infty^2(1-c)^2]^{\frac{1}{2}}\left(\frac{1}{\zeta}+\eta\right)\right\}, \tag{4.12}$$

where $K_n(z_1)$ denotes the modified Bessel function of order n, argument z_1, and the

sign is chosen such that the real part of the argument is positive to ensure boundedness as $\eta \to \infty$; ϕ_∞ is a constant. Equation (4.12) also leads to

$$p \sim \mp \frac{\phi_\infty M_\infty^2 \, \mathrm{i}\alpha(1-c) K_0\left\{\pm\alpha[1-M_\infty^2(1-c)^2]^{\frac{1}{2}}\left(\frac{1}{\zeta}+\eta\right)\right\}}{[1-M_\infty^2(1-c)^2]^{\frac{1}{2}}}. \tag{4.13}$$

The eigenvalue problem (for the temporal case as considered here) is then, for a given α, to find c subject to boundedness as $\eta \to \infty$, and such that the impermeability condition (4.10) is satisfied.

Before carrying out a detailed numerical study of this above eigenvalue problem, we turn to study an important condition relating to the existence of certain unstable eigensolutions.

5. The doubly generalized inflexion condition

In the case of compressible planar flows, the existence of the so-called generalized inflexion point, where (in our notation)

$$\frac{\mathrm{d}}{\mathrm{d}\eta}\left[\frac{w_{0\eta}}{T_0}\right] = 0, \tag{5.1}$$

is of great importance, as shown originally by Lees & Lin (1946) and confirmed by Reshotko (1962), Mack (1984, 1987) for example.

If condition (5.1) is satisfied at some point η_1, then there exists a neutral solution, with wavespeed c, such that

$$c = w_0(\eta_1), \tag{5.2}$$

provided

$$T_0 - M_\infty^2(w_0 - c)^2 > 0, \tag{5.3}$$

for all η.

This is a condition for the existence of a so-called neutral subsonic disturbance, i.e. for which

$$1 - 1/M_\infty < c < 1 + 1/M_\infty, \tag{5.4}$$

using the terminology described by Mack (1984), where sonic disturbances have

$$c = 1 \pm 1/M_\infty, \tag{5.5}$$

and supersonic disturbances have

$$c < 1 - 1/M_\infty \quad \text{or} \quad c > 1 - 1/M_\infty. \tag{5.6}$$

The condition (5.1) has a further important repercussion, namely that a condition for the existence of an amplified disturbance is that

$$\frac{\mathrm{d}}{\mathrm{d}\eta}\left[\frac{w_{0\eta}}{T_0}\right] = 0 \tag{5.7}$$

at some $\eta > \eta_c$, where η_c is the point at which

$$w_0(\eta) = 1 - 1/M_\infty. \tag{5.8}$$

The question that then arises is what is the effect of curvature on these important conditions? We address this question next. We take (4.9) as our starting point, and follow the general approach adopted in the past to tackle inflexional instabilities arising in planar compressible flows (e.g. Mack 1984), although here the situation is more complicated because of the inclusion of curvature terms.

Taking (4.9), dividing through by w_0-c, and multiplying by ϕ^* (where an asterisk denotes a complex conjugate) we obtain

$$\frac{\phi^*}{w_0-c}\frac{\mathrm{d}}{\mathrm{d}r}\left[\frac{(w_0-c)\left(\phi_r+\frac{1}{r}\phi_r\right)-w_{0r}\phi}{\chi}\right]=\frac{\alpha^2}{T_0}\phi\phi^*, \tag{5.9}$$

where
$$r = 1+\zeta\eta, \tag{5.10}$$

and
$$\chi = T_0-M_\infty^2(w_0-c)^2. \tag{5.11}$$

If we now subtract its complex conjugate from (5.9) we obtain

$$\frac{\phi^*}{w_0-c}\frac{\mathrm{d}}{\mathrm{d}r}\left[\frac{(w_0-c)\left(\phi_r+\frac{1}{r}\phi\right)-w_{0r}\phi}{\chi}\right]=\frac{\phi}{w_0-c^*}\frac{\mathrm{d}}{\mathrm{d}r}\left[\frac{(w_0-c^*)\left(\phi_r^*+\frac{1}{r}\phi^*\right)-w_{0r}\phi^*}{\chi^*}\right]. \tag{5.12}$$

After some algebra, this may be written as follows:

$$\phi^*\frac{\mathrm{d}}{\mathrm{d}r}\left[\frac{\phi_r+\frac{1}{r}\phi}{\chi}\right]-\phi\frac{\mathrm{d}}{\mathrm{d}r}\left[\frac{\phi_r^*+\frac{1}{r}\phi^*}{\chi^*}\right]=r\phi\phi^*\left\{\frac{1}{w_0-c}\frac{\mathrm{d}}{\mathrm{d}r}\left[\frac{w_{0r}}{\chi r}\right]-\frac{1}{w_0-c^*}\frac{\mathrm{d}}{\mathrm{d}r}\left[\frac{w_{0r}}{\chi^* r}\right]\right\}. \tag{5.13}$$

We now focus attention on the limit of the neutral state, i.e. if

$$c = c_r+\mathrm{i}c_i \tag{5.14}$$

then $c_i\to 0$.

We may write $\chi^*=\chi$ in this limit without any difficulty (assuming that the wave is not given by either of (5.5), which we shall see is outside of the scope of the following). However, we exert some care in the treatment of the right-hand side of (5.13), which we now write as

$$\frac{1}{r}\frac{\mathrm{d}}{\mathrm{d}r}\left[\frac{r\phi^*\left(\phi_r+\frac{1}{r}\phi\right)-r\phi\left(\phi_r^*+\frac{1}{r}\phi^*\right)}{\chi}\right]=\frac{2\mathrm{i}r|\phi|^2\mathrm{i}c_i}{|w_0-c|^2}\frac{\mathrm{d}}{\mathrm{d}r}\left(\frac{w_{0r}}{\chi r}\right). \tag{5.15}$$

We now use the following arguments: (i) as $c_i\to 0$, the derivative of the term in parentheses on the left-hand side of (5.15) is always zero, except possibly at the point r_i, where $w_0=c$; (ii) the term inside the parentheses must be zero at the wall ($r=1$), and asymptote to zero at infinity *if the wave is subsonic*; (iii) the right-hand side acts as a delta function at r_i as $c_i\to 0$, unless

$$\frac{\mathrm{d}}{\mathrm{d}r}\left(\frac{w_{0r}}{T_0 r}\right)_{r=r_i}=0, \tag{5.16}$$

or equivalently
$$\frac{\mathrm{d}}{\mathrm{d}\eta}\left[\frac{w_{0\eta}}{T_0(1+\zeta\eta)}\right]_{\eta=\eta_i}=0, \tag{5.17}$$

where
$$\eta_i = (r_i-1)/\zeta \tag{5.18}$$

(note $\chi(r=r_i)=T_0$). This condition is clearly required in order to avoid a finite jump in the term in parentheses on the left-hand side of (5.15), and the subsequent contradiction. Equation (5.16) may be viewed as a 'doubly generalized inflexion condition', and includes a curvature term, not present in planar studies.

We thus see that (5.16) is a necessary condition for the existence of so-called subsonic modes. In the following section we carry out a numerical study of the disturbance equations; as we shall see, (5.16) gives us an extremely useful guide to the behaviour, nature, and existence of the various modes of instability present.

6. Solution of disturbance equation

6.1. *Numerical method*

For the purposes of numerical solution, (4.7) and (4.8) were chosen (in preference to (4.9)). A fairly straightforward Runge–Kutta scheme was applied to this system, with the shooting commencing at some suitably large value of η, with (4.12) and (4.13), and the computation proceeding inwards, towards $\eta = 0$. The impermeability condition at $\eta = 0$ was satisfied by choosing the appropriate value of c (by means of Newton's method).

In a number of computations it was found advantageous to divert the computation below the real η-axis, in particular when $|w_0 - c|$ was small (if $\mathrm{Im}\{c\} \leqslant 0$ this procedure must be used). A similar technique has been used by Mack (1965), a method based on that of Zaat (1958).

6.2. *Doubly generalized inflexion point results*

Before presenting details for the eigenvalue problem *per se*, defined in §4, we return briefly to consider further results for the basic flow. It was shown in §5 how the so-called doubly generalized inflexion points are likely to play an important role in the stability of the flow. Consequently we return to consider the two examples studied in §3.2, namely $M_\infty = 2.8$ and $M_\infty = 3.8$. In particular we are interested in the existence of doubly generalized inflexion points.

Figure 3(*a*) (dotted line) shows the axial variation of position of the doubly generalized inflexion points for $M_\infty = 2.8$. The point $\zeta = 0$ corresponds to the leading edge of the cylinder, and as such corresponds to the planar case (as a result of our basic assumptions). There are two particularly striking features to this distribution: (i) that these points occur in pairs and (ii) there exists a critical value of ζ, downstream of which no such points exist. The upper points are an extension of the generalized inflexion point found important in planar cases, whilst the lower points rise off the surface of the cylinder $\eta = 0$, to ultimately merge with the upper branch at $\zeta \approx 0.059$. It is remarkable how the doubly generalized inflexion points disappear at such a small distance downstream of the leading edge.

It was also shown in §5 how neutral solutions with wavespeed

$$c = w_0(\eta_1) \tag{6.1}$$

will occur, provided

$$1 - 1/M_\infty < c < 1 + 1/M_\infty, \tag{6.2}$$

and so in figure 3(*b*) (dotted line) we show the axial distribution of $w_0(\eta_1)$ for $M_\infty = 2.8$. Because of the restriction (6.2) it is seen that subsonic inflexional modes of instability will only occur for $0 \leqslant \zeta \lesssim 0.047$, implying that such modes will completely disappear at just a distance approximately $0.0022C^{-1}Re$ body radii downstream of the leading edge (although other modes types are certainly possible); consequently in this case we expect this mode will disappear before the doubly generalized inflexion points have merged. There are certain similarities here with the effect of cooling of planar boundary layers (Lees 1947; Mack 1987), which causes a similar effect on generalized inflexion points.

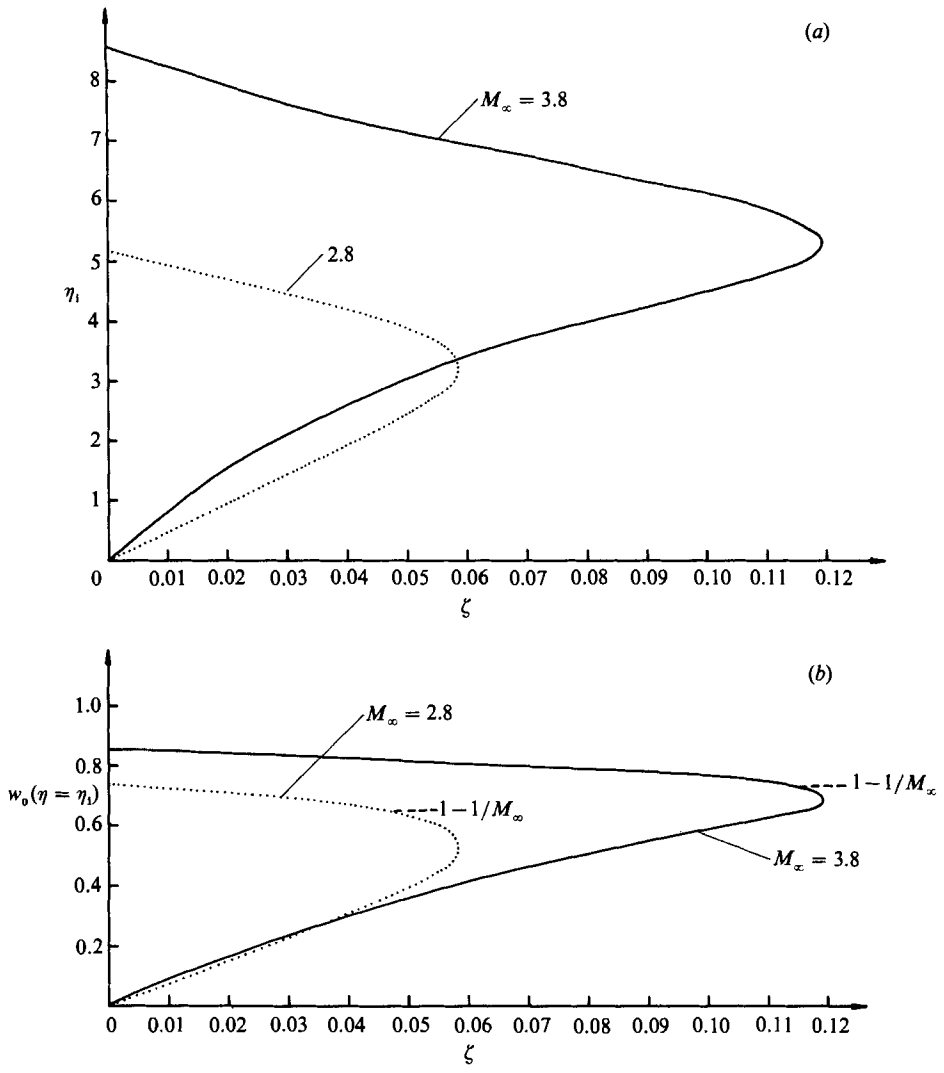

FIGURE 3. (*a*) Variation of transverse positions of inflexion points (η_i) with axial location ζ. (*b*) Variation of $w_0(\eta = \eta_i)$ with ζ.

We next turn our attention to results for the higher Mach number considered previously, $M_\infty = 3.8$. Figure 3(*a*) (solid line) shows the axial variation of the doubly generalized inflexion points in this case; the general characteristics are the same as those for $M_\infty = 2.8$ except that the range of ζ for which such points exist is increased. The corresponding distribution of $w_0(\eta_i)$ is shown in figure 3(*b*) (solid line); this too is similar to the corresponding $M_\infty = 2.8$ distribution also shown in figure 3(*b*). In the case of $M_\infty = 3.8$, figure 3(*b*) indicates that neutral subsonic inflexional modes will disappear a distance approximately $0.013C^{-1}Re$ body radii downstream of the leading edge.

We see that the ζ-point at which the two inflexion points merge moves significantly further downstream as the Mach number increases. We expect this trend to continue unabated as the Mach number increases, since (as shown by Mack 1987) the η-

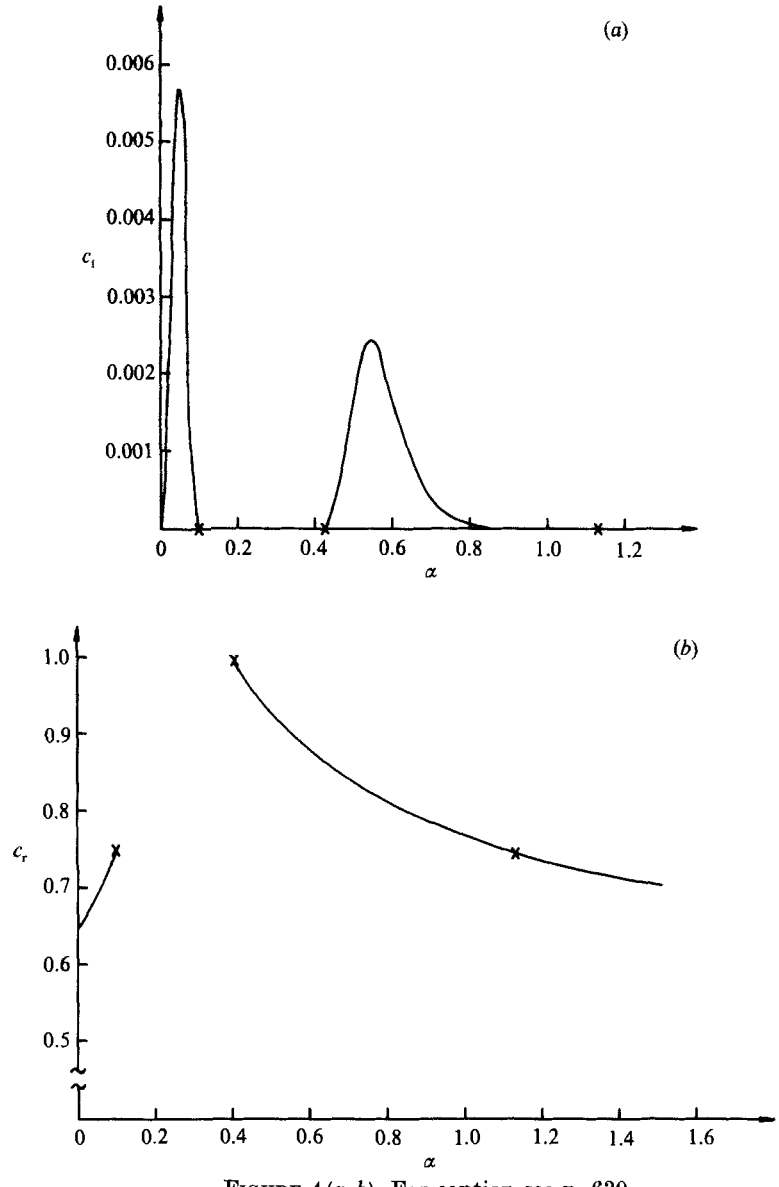

FIGURE 4(*a*, *b*). For caption see p. 630.

position of the (planar) generalized inflexion point moves continuously outward with an increase in M_∞.

Guided by the above observations, we now turn our attention to the eigenvalue problem for the two cases $M_\infty = 2.8$ and $M_\infty = 3.8$.

6.3. *Growth rate results*

Figure 4(*a*) shows the variation of c_i with α (where $c = c_r + ic_i$), for the case $M_\infty = 2.8$, at $\zeta = 0$ (and hence corresponds to a planar example). The corresponding results for c_r are shown in figure 4(*b*). Here, and in all results to follow, neutral points are denoted by a cross. These results (which are typical of previous planar results – see

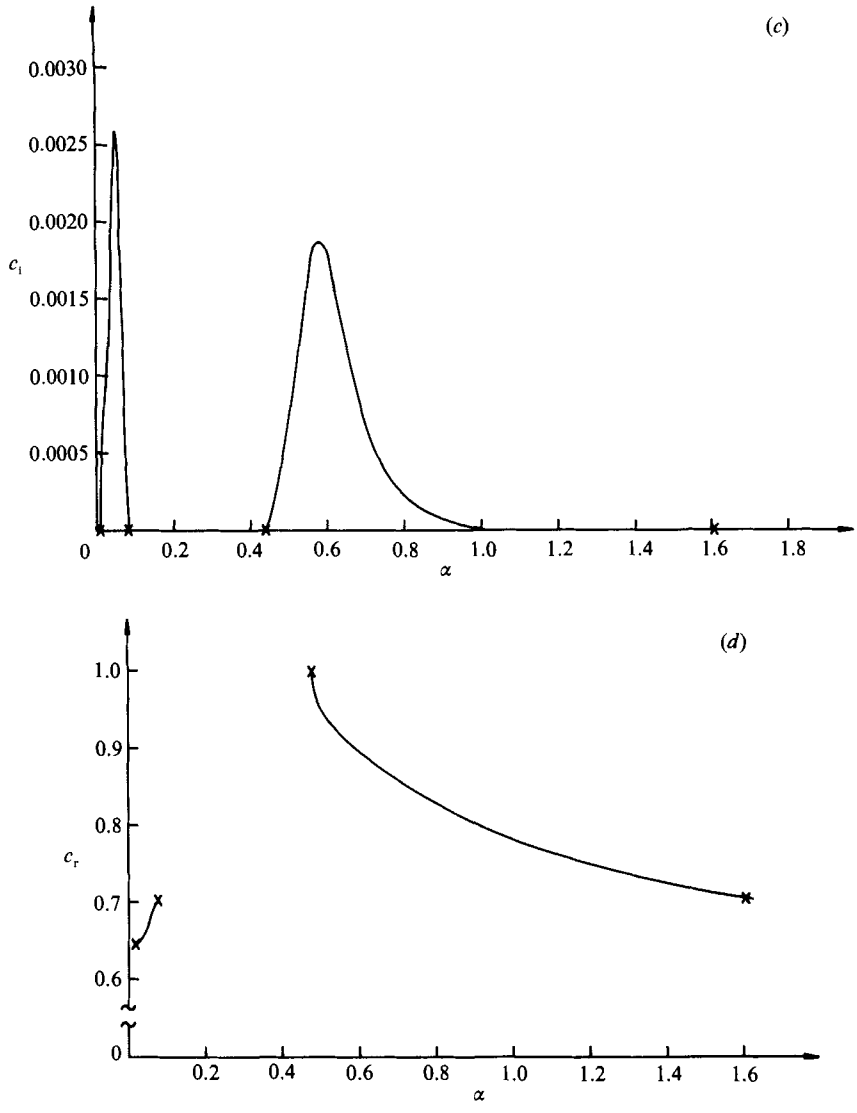

FIGURE 4(*c*, *d*). For caption see p. 630.

for example Mack 1987) show two distinct unstable modes. The first (to be referred to as mode I) originates as a sonic neutral disturbance (with $c_i = 0$, $c_r = 1 - 1/M_\infty$) at $\alpha = 0$, and terminates as a neutral inflexional subsonic mode at $\alpha \approx 0.1$, where $c_r = w_0(\eta = \eta_i) \approx 0.66$; this mode in fact continues, becoming a decaying mode, with $c_i < 0$, although we shall mainly concentrate our attention on growing/neutral modes).

The second mode (to be referred to as mode II) originates at $\alpha \approx 0.4$ as a subsonic neutral mode with $c_i = 0$, $c_r = 1$ (this may be regarded as a special case of an inflexional mode, with the generalized inflexion point occurring in the free stream). This mode then terminates at $\alpha \approx 1.13$ as a (second) neutral subsonic inflexional instability (and at values of α greater than this value continues as a decaying mode, with $c_i < 0$).

Although other modes of instability undoubtedly exist at this Mach number, these

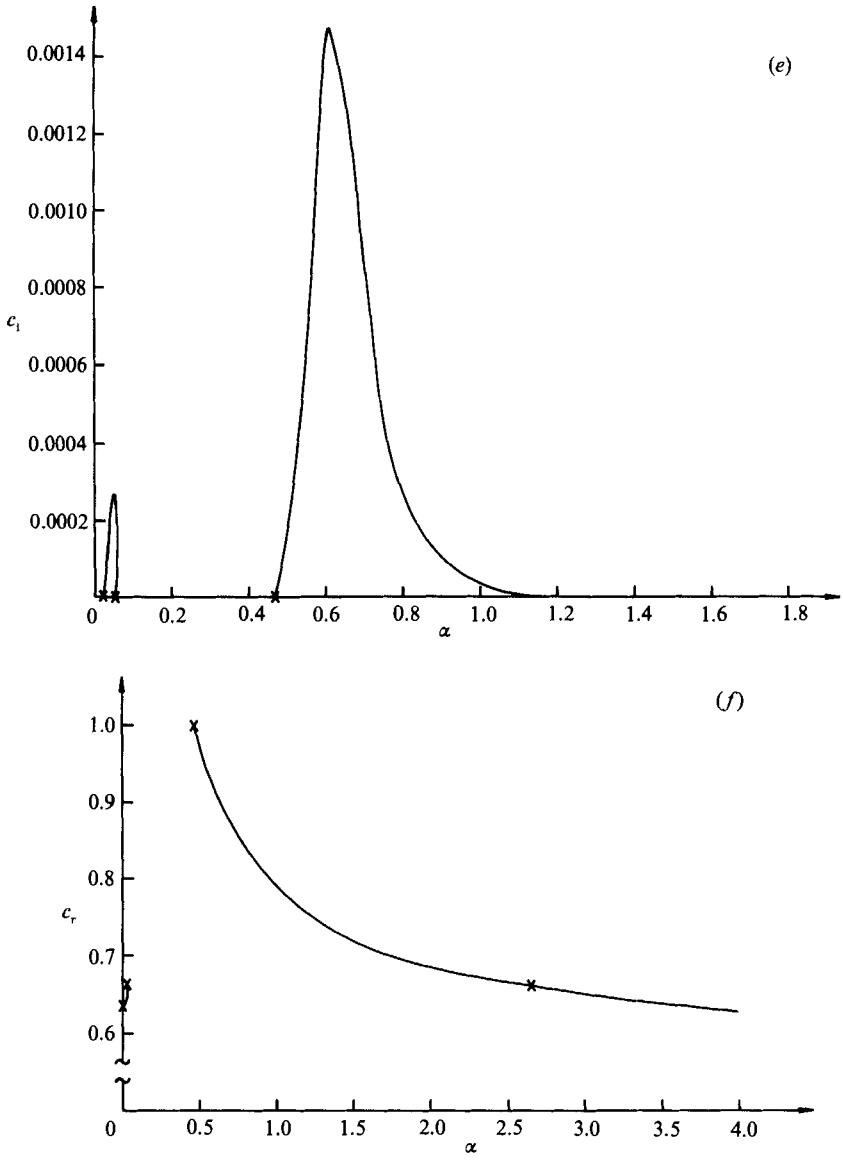

FIGURE 4(*e*,*f*). For caption see p. 630.

have considerably smaller growth rates than modes I and II shown here, and are consequently much less important from a practical point of view. Note that since the (temporal) growth rate is αc_i, mode II is the most important.

We now turn to results incorporating the effects of curvature. Figures 4(*c*) and 4(*d*) show distributions of c_i and c_r (respectively), with α (for $M_\infty = 2.8$), at $\zeta = 0.02$. Although the qualitative features resemble those of the $\zeta = 0$ case, the maximum of the growth rates is seen to be considerably reduced (in spite of the smallness of ζ), particularly that of mode I.

A further effect of curvature, just perceptible, is that the lower limit of mode I, which in the planar case corresponds to a sonic neutral mode, with $\alpha = 0$ and $c = 1 - 1/M_\infty$, is slightly shifted along the α-axis, being neutral at a very small positive

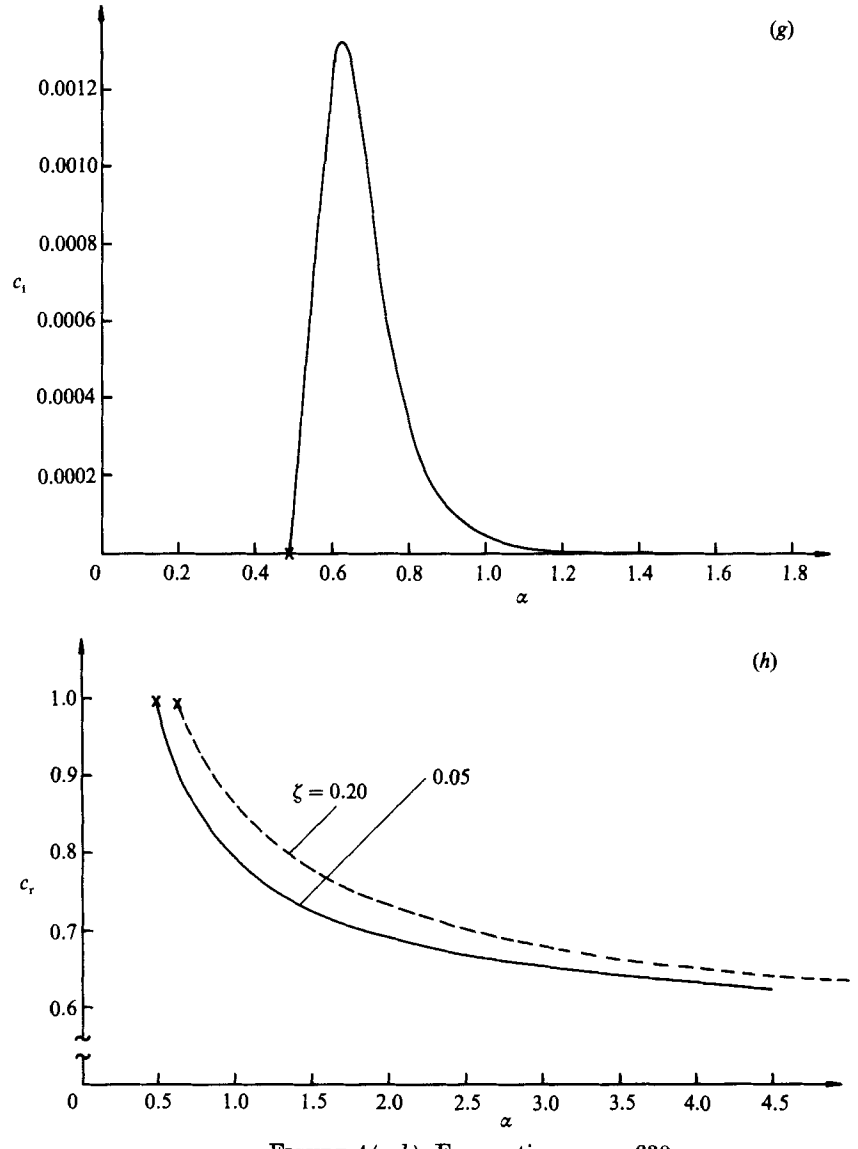

FIGURE 4(*g*, *h*). For caption see p. 630.

value of α. Although the c_r at this point was very close to being sonic, the indications from the computations were that this lower neutral point had become very slightly supersonic.

Moving further down the axis of the cylinder, to $\zeta = 0.04$, figures 4(*e*) (c_i distribution) and 4(*f*) (c_r distribution) indicate that mode I has practically disappeared, whilst the maximum growth rate of mode II is now significantly diminished, terminating (at a subsonic inflexional neutral point) at quite a large value of α (≈ 2.65), although over much of the range of α this mode has exceedingly small growth rates. The computations also indicate that the lower neutral point of mode I has moved further along the real α-axis (compared to the $\zeta = 0.02$ results).

Following our comments in the previous subsection regarding $w_0(\eta_1)$ dropping below $1 - 1/M_\infty$, we expect mode I to completely disappear at $\zeta \approx 0.047$ for this

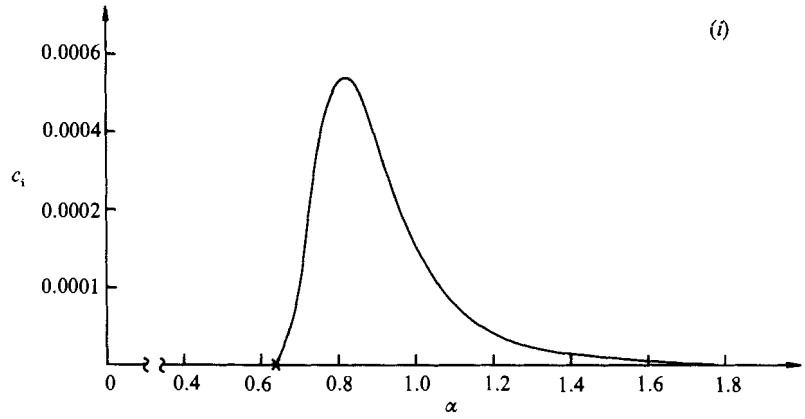

FIGURE 4. (*a*) Variation of c_i with α, $\zeta = 0$ (planar case). (*b*) Variation of c_r with α, $\zeta = 0$ (planar case). (*c*) Variation of c_i with α, $\zeta = 0.02$. (*d*) Variation of c_r with α, $\zeta = 0.02$. (*e*) Variation of c_i with α, $\zeta = 0.04$. (*f*) Variation of c_r with α, $\zeta = 0.04$. (*g*) Variation of c_i with α, $\zeta = 0.05$. (*h*) Variation of c_r with α, $\zeta = 0.05$ and $\zeta = 0.2$. (*i*) Variation of c_i with α, $\zeta = 0.2$. $M_\infty = 2.8$.

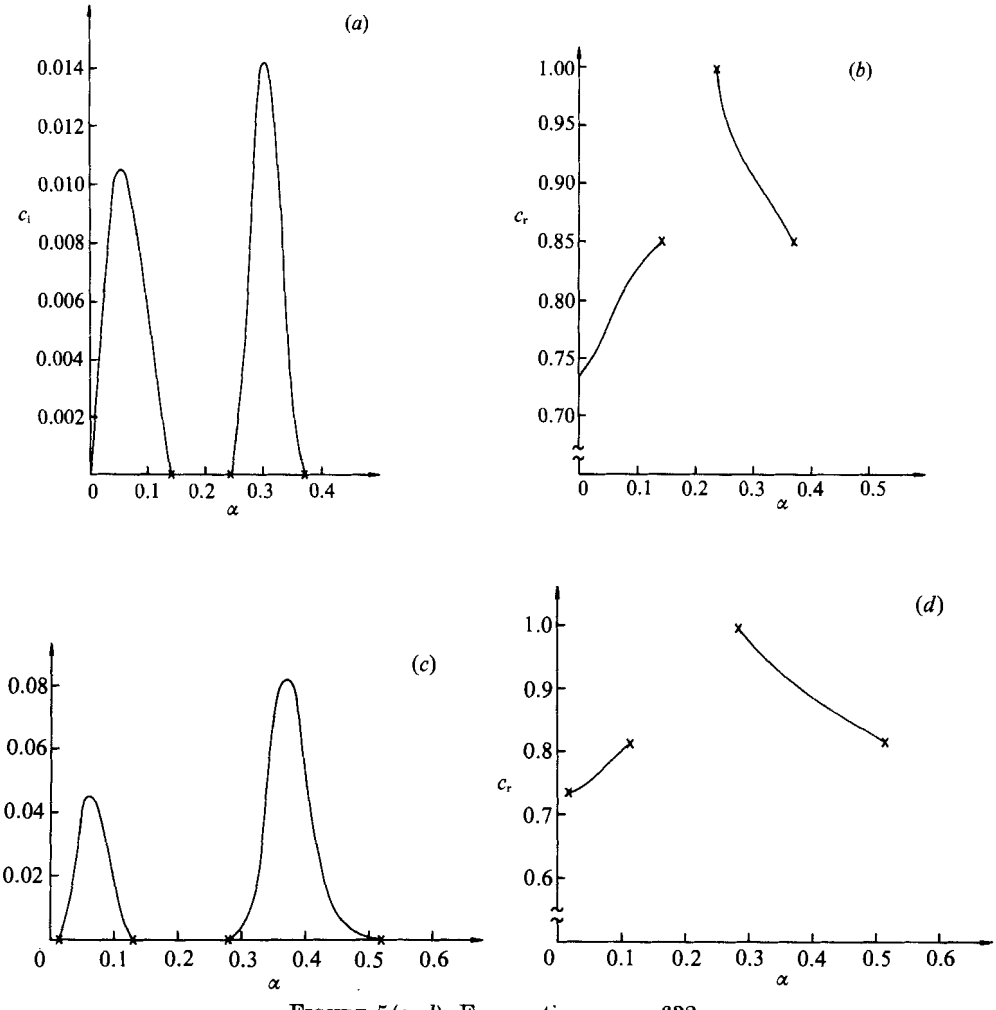

FIGURE 5(*a–d*). For caption see p. 632.

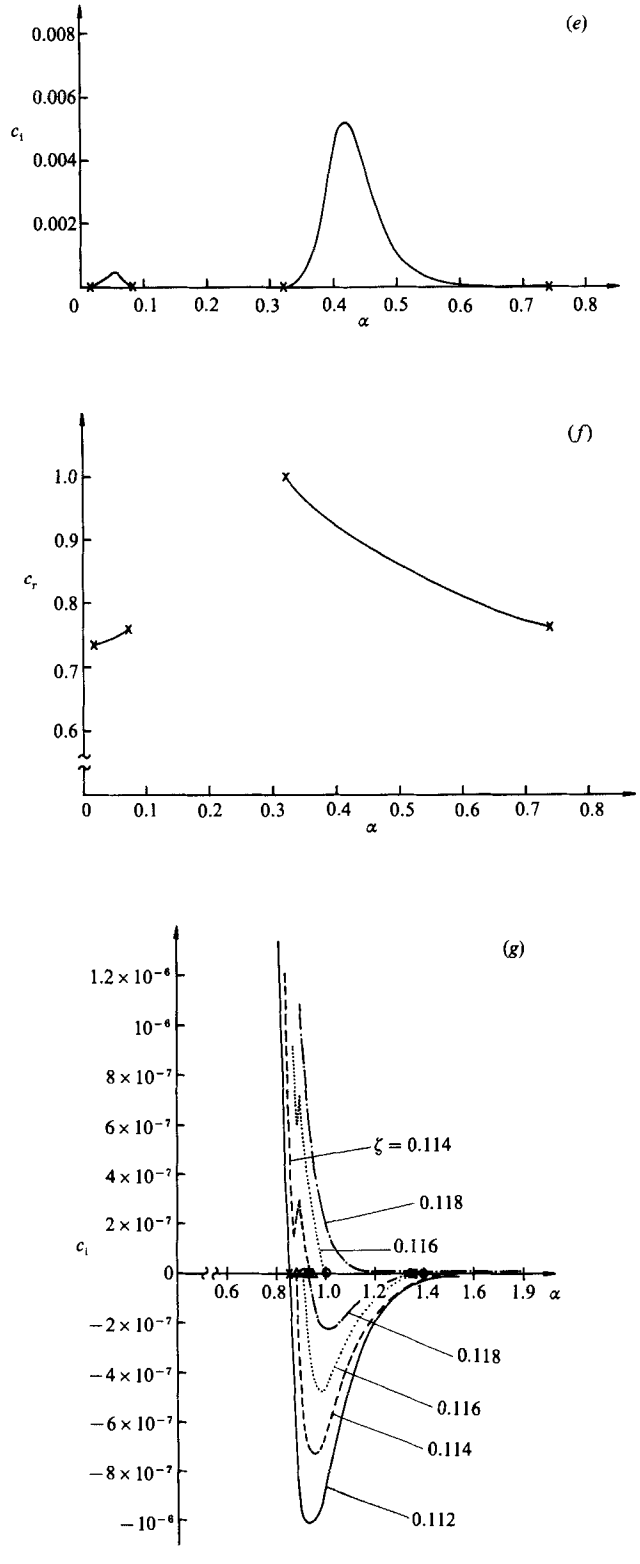

FIGURE 5(*e–g*). For caption see p. 632.

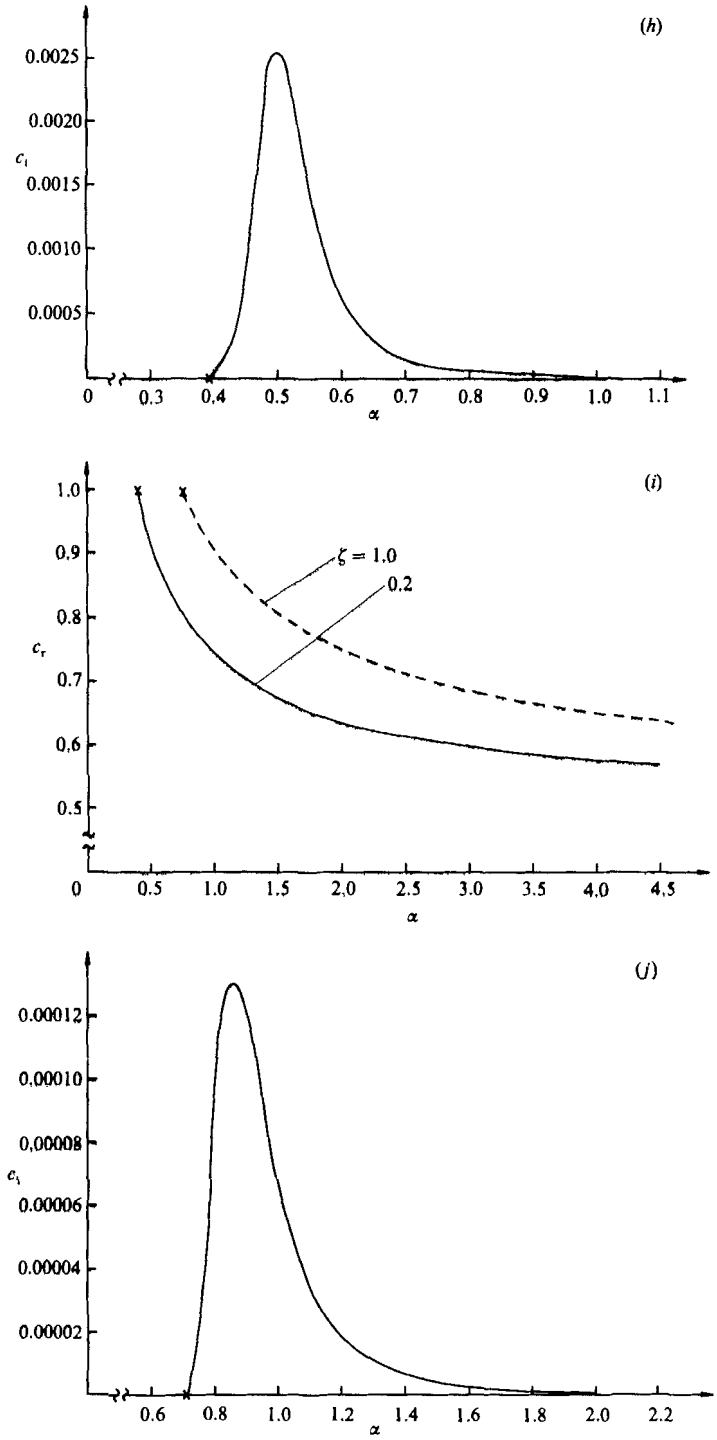

FIGURE 5. (*a*) Variation of c_i with α, $\zeta = 0$ (planar case). (*b*) Variation of c_r with α, $\zeta = 0$ (planar case). (*c*) Variation of c_i with α, $\zeta = 0.05$. (*d*) Variation of c_r with α, $\zeta = 0.05$. (*e*) Variation of c_i with α, $\zeta = 0.1$. (*f*) Variation of c_r with α, $\zeta = 0.1$. (*g*) Variation of c_i with α, $\zeta = 0.112$, 0.114, 0.116, 0.118. (*h*) Variation of c_i with α, $\zeta = 0.2$. (*i*) Variation of c_r with α, $\zeta = 0.2$ and $\zeta = 1.0$. (*j*) Variation of c_i with α, $\zeta = 1.0$. $M_\infty = 3.8$.

choice of M_∞. As a consequence, the next set of results (at $\zeta = 0.05$) presented in figures 4(*g*) (c_i) and 4(*h*) (c_r, shown as a solid line) shows just mode II, which itself exhibits a further reduction in growth rate. This mode still originates as a neutral mode with $c_r = 1$ (at $\alpha \approx 0.45$); unfortunately our computations did not indicate a clear neutral solution at an upper value of α. This was due to the exceedingly small growth rates encountered, which were typically $O(10^{-10})$, and hence were comparable with the round-off associated with the computation. (In the regime of larger α and very small growth rates, it was found to be most essential to deform the integration contour in the numerical scheme, as described in §6.1, in order to maintain numerical accuracy.) If a neutral point exists, as seems likely, it must be of the neutral supersonic class ($c_i = 0$, $c_r < 1 - 1/M_\infty$) because of the absence of any doubly generalized inflexion points at this value of ζ.

As a final example of the $M_\infty = 2.8$ flow, we show results for $\zeta = 0.2$ in figures 4(*i*) (c_i) and 4(*h*) (c_r) drawn as a broken line. These indicate qualitative similarity with the previous set of results; however, the maximum growth rate is reduced by approximately an order of magnitude. Again, unfortunately, positive identification of an upper neutral point was not possible, owing to the difficulties with tiny growth rates encountered at larger values of α. We conclude, however, that curvature has important (and profound) effects: (i) annihilation of mode I and (ii) substantial reduction of the growth rate of mode II (although the range of α over which this unstable mode exists is increased quite significantly).

We next turn our attention to results for $M_\infty = 3.8$, and figures 5(*a*) and 5(*b*) show c_i and c_r distributions (respectively) with α, for the particular case $\zeta = 0$. This corresponds to the planar case as computed previously (Mack 1987 for example) and thus provides a useful check on the accuracy of the present overall scheme (which is seen to be entirely satisfactory). When compared with the corresponding $M_\infty = 2.8$ results (figure 4*a*, *b*), the importance of mode II is seen to be significantly increased (although the growth rate of mode I is increased also). Generally, the $M_\infty = 3.8$ distributions qualitatively resemble the corresponding $M_\infty = 2.8$ distributions.

At $\zeta = 0.05$ (with $M_\infty = 3.8$), we see in figures 5(*c*) (c_i distribution) and 5(*d*) (c_r distribution) that there is an approximate halving of the maximum growth rate, when compared with the $\zeta = 0$ results. The results also indicate that the lower neutral point of mode I has moved along the positive real axis, and has (just as in the $M_\infty = 2.8$ example) become very slightly supersonic. Further downstream, at $\zeta = 0.10$ (figures 5*e*, *f*) mode I has almost disappeared, whilst mode II has suffered a further depletion of maximum growth rate.

From our observations made in §6.2, we expect that mode I will completely disappear at $\zeta \approx 0.013$ (where $c_r = w_0(\eta = \eta_i) = 1 - 1/M_\infty$); this will also be an important location for the upper neutral point of mode II, which for $\zeta \leqslant 0.013$ is of the subsonic inflexional kind. As noted earlier, for the previous M_∞ considered, growth rates in this regime were extremely small, and so no firm conclusions on the behaviour of this mode in this region were possible. Fortunately, although the growth rates in this critical region at $M_\infty = 3.8$ are small, they are nonetheless significantly larger than at the lower Mach number.

The solid line in figure 5(*g*) details the *local* variation of c_i with α at $\zeta = 0.112$ (just below the critical value). Mode II is clearly seen to become damped at $\alpha \approx 0.85$, with $|c_i|$ reaching a maximum at $\alpha \approx 0.93$, and then decreasing. Unfortunately, no firm conclusions are possible regarding the ultimate behaviour of c_i at large values of α, owing to the smallness of $|c_i|$.

The dashed line in figure 5(*g*) represents the distribution of c_i in the same critical

region of α, at $\zeta = 0.114$ (slightly above the critical value of ζ). It now appears that the growing mode II terminates at $\alpha \approx 0.94$, as a supersonic neutral mode, *and does not continue as a damped mode.* (The kink observed on this section of the curve was confirmed by numerical experimentation.) Instead, a further (supersonic) neutral mode has already appeared (at $\alpha \approx 0.88$) and this is then the origin of a damped mode, which has a maximum value of $|c_i|$ at $\alpha \approx 0.95$; $|c_i|$ then decreases towards zero, and again because of its ultimate smallness, no conclusions regarding its behaviour at larger values of α are possible. Additionally, there was some evidence of another unstable mode, beginning at around $\alpha \approx 1.52$, but because of its very small growth rate it is not possible to be completely categorical about this; its growth rate was also too small to be seen on the scale of figure 5(*h*). Thus in this case we see the presence of possibly three (supersonic) neutral points in this regime.

The dotted line in figure 5(*g*) details the variation of c_i in the crucial α-region, for the location $\zeta = 0.116$. Again, (growing) mode II is seen to terminate at a supersonic neutral point, this time located at $\alpha \approx 1$. The kink on this section of the curve was again checked numerically. A further supersonic neutral point exists, originating at $\alpha \approx 0.9$ which then provides the start for a decaying mode; when compared to the corresponding $\zeta = 0.114$ mode, the decay rate of this particular mode is seen to be reduced. Further, this mode now seems to terminate at another neutral point (at $\alpha \approx 1.48$). Yet another neutral point exists at $\alpha \approx 1.40$, which then provides the start of a second unstable mode (although the growth rate of this mode was so small as to be barely visible on figure 5*g*); a total of four supersonic neutral points are thus observed in this region of α.

The dot-dashed line in figure 5(*g*) shows the c_i distribution at $\zeta = 0.118$ in the same general region of α. When compared with the previous results, a further change to the qualitative picture is seen. Here, the original mode II has merged with the second unstable mode. Just two neutral points remain in this region, at $\alpha \approx 0.93$ and $\alpha \approx 1.35$, which are associated with the start and the terminus of the decaying mode (which generally has a significantly reduced $|c_i|$ compared to the previous results). The ultimate behaviour of the growing mode with α remains unclear, owing to the smallness of $|c_i|$.

It is interesting to note that when two modes were present (for a given value of α), both modes had values of c_r that were practically indistinguishable. Further, there was no difficulty in calculating accurate values of c_r, even at large values of α.

Moving further downstream to $\zeta = 0.2$, the decaying mode has disappeared completely, and c_i and c_r distributions over a broad range of α are shown in figures 5(*h*) and 5(*i*) (solid line) respectively. When compared with the figure 5(*e*) results, the mode II growth rates are quite appreciably reduced; the ultimate behaviour of $|c_i|$ at large values of α remains unclear.

Further downstream still, at $\zeta = 1.0$, the results (c_i shown in figure 5(*j*), c_r shown in figure 5(*i*) as a dashed line) are qualitatively similar to those at $\zeta = 0.2$, except that the maximum value of c_i is significantly diminished, and occurs at a rather larger value of α (as does the origin of this mode which occurs at $\alpha \approx 0.72$, compared with $\alpha \approx 0.4$ in the case of $\zeta = 0.2$). The larger-α behaviour of this mode is again unclear, because of the reasons described above.

In the following section we consider a number of general conclusions and points raised by this work.

7. Conclusions

In this paper the supersonic flow over a thin straight circular cylinder has been investigated. The basic boundary-layer flow has been obtained, and the inviscid stability of the flow has been studied. A condition on the basic flow for the existence of so-called subsonic inflexional neutral modes of instability has been derived, and is found to be an extension of the generalized inflexional condition relevant to planar flows.

The effect of body surface curvature is seen to immediately (and significantly) reduce the importance of the 'first mode' of inviscid instability, which is seen to completely disappear at what could be a comparatively short distance down the axis of the cylinder (by about $0.0022C^{-1}Re$ body radii at $M_\infty = 2.8$, and by about $0.013C^{-1}Re$ body radii at $M_\infty = 3.8$).

The maximum growth rate of the 'second mode' of inviscid instability also suffers a substantial reduction at locations increasingly further down the axis of the cylinder, although the evidence is that it does not disappear completely.

It is also useful to note that since in many cases computed the temporal growth rate is small, although the study here has been entirely confined to temporal instabilities, the transformation of Gaster (1962) could be expected to yield reasonably accurate estimates for the corresponding spatial instability problem.

There are certain similarities here with the effect of cooling a planar boundary layer (Mack 1984, 1987, for example), which can also cause the first mode to disappear completely (cooling also causes the formation of a second generalized inflexion point, which with a progressive reduction in wall temperature eventually coalesces with the first generalized inflexion point). However, the effect of cooling is to increase the amplification rate of the second mode (in contrast to our results featuring curvature).

It is particularly interesting to note that although inviscid modes of instability are generally regarded as more important/unstable than viscous modes of instability in the case of supersonic planar flows, the work of Duck & Hall (1989, 1990) on viscous axisymmetric flows indicates that a reduction in body radius (equivalent to a further downstream location in our context) causes an increase in amplification rate. Thus it is entirely possible that with axisymmetric flows, regimes may exist where viscous instability is dominant.

It is to be hoped that this study will provide a basis for the study of flows over further and more practical geometries, such as cones. One important omission from the physics of that problem, which must ultimately be resolved, is the exclusion of any shock waves in the basic flow (however, this may be justified by the restriction of thinness), although previous works on planar flows (cited throughout this paper) all have this same omission. It is also hoped that these results will provide material for comparison with finite-Reynolds-number computations.

Finally, here just axisymmetric modes have been considered and it may well be that non-axisymmetric modes are important; this aspect is currently under investigation.

This research was supported by the National Aeronautics and Space Administration under NASA contracts No. NAS1-18605 and NAS1-18107 while the author was in residence at the Institute for Computer Applications in Science and Engineering (ICASE), NASA Langley Research Center, Hampton, VA 23665.

The author wishes to thank Mr Stephen Shaw (University of Manchester) for a

number of useful comments on this work. A number of computations were carried out at the University of Manchester Computer Centre with computer time provided under SERC Grant number GR/E/25702.

REFERENCES

BROWN, W. B. 1962 Exact numerical solutions of the complete linearized equations for the stability of compressible boundary layers. *Norair Rep.* NOR-62-15. Northrop Aircraft Inc., Hawthorne, LA.

BUSH, W. B. 1976 Axial incompressible viscous flow past a slender body of revolution. *Rocky Mountain J. Maths* **6**, 527.

DUCK, P. W. & BODONYI, R. J. 1986 The wall jet on an axisymmetric body. *Q. J. Mech. Appl. Maths* **39**, 407.

DUCK, P. W. & HALL, P. 1989 On the interaction of axisymmetric Tollmien–Schlichting waves in supersonic flow. *Q. J. Mech. Appl. Maths* **42**, 115 (also *ICASE Rep.* 88-10).

DUCK, P. W. & HALL, P. 1990 Non-axisymmetric viscous lower branch modes in axisymmetric supersonic flows. *J. Fluid Mech.* **213**, 191–201. (Also *ICASE Rep.* 88-42).

GASTER, M. 1962 A note on the relation between temporally-increasing and spatially-increasing disturbances and hydrodynamic stability. *J. Fluid Mech.* **14**, 222.

GLAUERT, M. B. & LIGHTHILL, M. J. 1955 The axisymmetric boundary layer on a long thin cylinder. *Proc. R. Soc. Lond.* A **230**, 188.

KÜCHEMANN, D. 1938 Störungsbewegunyen in einer Gasströmung mit Grentschicht. *Z. Angew. Math. Mech.* **18**, 207.

LEES, L. 1947 The stability of the laminar boundary layer in a compressible fluid. *NACA Tech. Rep.* 876.

LEES, L. & LIN, C. C. 1946 Investigation of the stability of the laminar boundary layer in a compressible fluid. *NACA Tech. Note* 1115.

LIN, C. C. 1945*a* On the stability of two-dimensional parallel flows, part I. *Q. Appl. Maths* **3**, 117.

LIN, C. C. 1945*b* On the stability of two-dimensional parallel flows, part II. *Q. Appl. Maths* **3**, 218.

LIN, C. C. 1945*c* On the stability of two-dimensional parallel flows, part III. *Q. Appl. Maths* **3**, 277.

MACK, L. M. 1963 The inviscid stability of the compressible laminar boundary layer. In *Space Programs Summary*, no. 37-23, p. 297. JPL, Pasadena, CA.

MACK, L. M. 1964 The inviscid stability of the compressible laminar boundary layer: Part II. In *Space Programs Summary*, no. 37-26, vol. IV, p. 165. JPL Pasadena, CA.

MACK, L. M. 1965*a* Stability of the compressible laminar boundary layer according to a direct numerical solution. *AGARDograph*, vol. 97, part I, p. 329.

MACK, L. M. 1965*b* Computation of the stability of the laminar boundary layer. In *Methods in Computational Physics* (ed. B. Alder, S. Fernbach & M. Rotenberg), vol. 4, p. 247. Academic.

MACK, L. M. 1969 Boundary-layer stability theory. *Document* 900-277, Rev. A. JPL, Pasadena, CA.

MACK, L. M. 1984 Boundary-layer linear stability theory. In *Special Course on Stability and Transition of Laminar Flow, AGARD Rep.* 709, p. 3-1.

MACK, L. M. 1987 Review of compressible stability theory. In *Proc. ICASE Workshop on the Stability of Time Dependent and Spatially Varying Flows.* Springer.

MICHALKE, A. 1971 Instabilität eines Kompressiblen rundens Freistrahls unter Berucksichtingung des Einflusses den Strahlgrenzschtdicke. *Z. Flugwiss.* **19**, 319.

MOORE, F. K. 1955 Unsteady laminar boundary layer flow. *NACA Tech. Note* 2471.

RESHOTKO, E. 1962 Stability of three-dimensional compressible boundary layers. *NASA Tech. Note* D-1220.

SEBAN, R. A. & BOND, R. 1951 Skin friction and heat transfer characteristics of a laminar boundary layer of a cylinder in axial incompressible flow. *J. Aero. Sci.* **10**, 671.

STEWARTSON, K. 1951 On the impulsive motion of a flat plate in a viscous fluid. *Q. J. Mech. Appl. Maths* **4**, 182.

STEWARTSON, K. 1955 The asymptotic boundary layer on a circular cylinder in axial incompressible flow. *Q. Appl. Maths* **13**, 113.

STEWARTSON, K. 1964 *The Theory of Laminar Boundary Layers in Compressible Fluids.* Oxford University Press.

THOMPSON, P. A. 1972 *Compressible Fluid Dynamics.* McGraw-Hill.

ZAAT, J. A. 1958 Numerische Beiträge zur Stabilitätstheoric de Grenzschichten. *Grenzschichtforschung Symp., IUTAM*, p. 127. Springer.